NANO LETTERS

Subscriber access provided by MICHIGAN STATE UNIVERSITY | MSU LIBRARIES

Letter

Electronic and Structural Characteristics of Zinc-Blende Wurtzite Biphasic Homostructure GaN Nanowires

Benjamin W. Jacobs, Virginia M. Ayres, Mihail P. Petkov, Joshua B. Halpern, Maoqi He, Andrew D. Baczewski, Kaylee McElroy, Martin A. Crimp, Jiaming Zhang, and Harry C. Shaw

Nano Lett., **2007**, 7 (5), 1435-1438 • DOI: 10.1021/nl062871y

Downloaded from http://pubs.acs.org on December 16, 2008

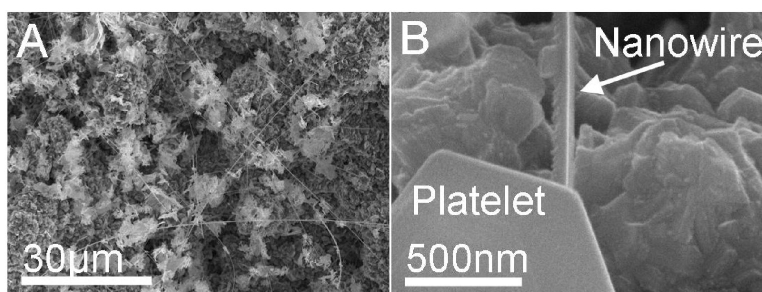

More About This Article

Additional resources and features associated with this article are available within the HTML version:

- Supporting Information
- Links to the 2 articles that cite this article, as of the time of this article download
- Access to high resolution figures
- Links to articles and content related to this article
- Copyright permission to reproduce figures and/or text from this article

View the Full Text HTML

ACS Publications
High quality. High impact.

Nano Letters is published by the American Chemical Society. 1155 Sixteenth Street N.W., Washington, DC 20036

NANO LETTERS

2007
Vol. 7, No. 5
1435−1438

Electronic and Structural Characteristics of Zinc-Blende Wurtzite Biphasic Homostructure GaN Nanowires

Benjamin W. Jacobs,[*,†] Virginia M. Ayres,[†] Mihail P. Petkov,[‡] Joshua B. Halpern,[§] Maoqi He,[§] Andrew D. Baczewski,[†] Kaylee McElroy,[†] Martin A. Crimp,[⊥] Jiaming Zhang,[⊥] and Harry C. Shaw[||]

Department of Electrical and Computer Engineering, Michigan State University, 2120 Engineering Building, East Lansing, Michigan 48824, Jet Propulsion Laboratory, Pasadena, California 91109, Department of Chemistry, Howard University, Washington, D.C. 20059, Department of Chemical Engineering and Materials Science, Michigan State University, East Lansing, Michigan 48824, and NASA Goddard Space Flight Center, Greenbelt, Maryland 20771

Received December 7, 2006; Revised Manuscript Received March 21, 2007

ABSTRACT

We report a new biphasic crystalline wurtzite/zinc-blende homostructure in gallium nitride nanowires. Cathodoluminescence was used to quantitatively measure the wurtzite and zinc-blende band gaps. High-resolution transmission electron microscopy was used to identify distinct wurtzite and zinc-blende crystalline phases within single nanowires through the use of selected area electron diffraction, electron dispersive spectroscopy, electron energy loss spectroscopy, and fast Fourier transform techniques. A mechanism for growth is identified.

Over the past decade, nanowires made from a wide variety of materials have demonstrated excellent electronic and chemical characteristics. Gallium nitride (GaN) nanowires in particular have shown potential for a wide range of optical and electronic devices as well as mechanical[1] applications. Room-temperature UV lasing has been reported for GaN nanowire systems.[2] GaN nanowire field effect transistors[3] and logic devices[4] have shown desirable characteristics such as high transconductance and good switching. Several device fabrication methods have also been realized, including directional catalyst growth[5,6] and focused ion beam metal deposition.[7−9]

Various methods have been employed for growing GaN nanowires including chemical vapor deposition (CVD),[10] metal-organic CVD (MOCVD),[11] growth within a carbon nanotube,[12] and laser ablation.[13] A metal catalyst is commonly used to initiate growth, and different growth directions have been achieved with different catalyst particles.[14] Catalyst-free GaN nanowire growth via molecular beam expitaxy and a vapor−liquid process has also recently been reported[15,16] and employs a growth mechanism similar to that described in the present study.

In these experiments, GaN nanowires are grown by a catalyst-free, vapor−liquid process from the direct reaction of Ga metal vapor with ammonia (NH_3) in a quartz tube furnace.[17,18] An amorphous GaN matrix forms first, followed by the appearance of small hexagonal platelets. By varying the ammonia flow rate (20−150 sccm) and temperature (800−1100 °C), the onset of nanowire growth and the diameters of the nanowires, which range from 10 nm to 10 μm, can be controlled. A study of the temperature-composition parameter space provides a predictive model for nanowire growth.[19] The nanowire length is determined by the duration of the growth cycle and can be millimeters in length. They form a single seamless structure along well-defined crystal axes. Scanning electron microscopy (Hitachi S-4700-II FESEM) images of the as-grown GaN nanowire/amorphous/platelet matrix and the nanowire from platelet growth are shown in Figure 1A,B. A relatively high density of nanowires is typically observed on the matrix surface.

In preparing the samples for cathodoluminescence and high-resolution transmission electron microscopy (HRTEM), the GaN nanowire/amorphous/platelet matrix was ultrasonicated in ethanol for 5 s to separate the nanowires from the amorphous/platelet matrix. The mixture was then separated by centrifuging the solution at ∼1000 rpm for 30 s and

* Corresponding author. E-mail: jacobsbe@egr.msu.edu.
† Department of Electrical and Computer Engineering, Michigan State University.
‡ Jet Propulsion Laboratory.
§ Department of Chemistry, Howard University.
⊥ Department of Chemical Engineering and Materials Science, Michigan State University.
|| NASA Goddard Space Flight Center.

10.1021/nl062871y CCC: $37.00 © 2007 American Chemical Society
Published on Web 04/07/2007

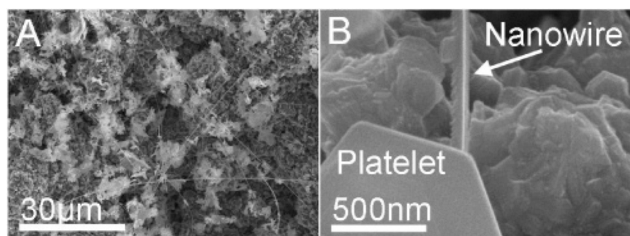

Figure 1. (A) SEM image of the distribution of nanowires on the growth matrix. (B) SEM image of a nanowire growing from a hexagonal platelet.

decanting, thereby eliminating most of the amorphous/platelet matrix from the solution. For the cathodoluminescence analysis, nanowires were dispersed on a silicon wafer with a layer of native oxide. For the HRTEM analysis, a small droplet of the ethanol/nanowire solution was placed on a copper TEM grid with either a carbon holey film or carbon lacy film spanning the holes of the grid and allowed to dry.

Cathodoluminescence (CL) experiments were performed in a LEO Supra 50 VP SEM in conjunction with a Gatan MonoCL system with a low-noise Peltier-cooled Hamamatsu R5509 photomultiplier detector. The GaN signature in the 290−360 nm wavelength range was used to optimize the CL signal. The best peak-to-background ratio was achieved at approximately 10 keV incident electron energy. The slit widths were set at 1 mm, which was the optimum for achieving high count rates, while maintaining sufficient resolution to differentiate between the wurtzite and zinc-blende band gaps. Narrower slits did not change the peak widths significantly. In these initial investigations, detailed analysis of the near band gap exciton electronic structure was not considered, and the experiments were carried out at room temperature.

The CL spectra of various GaN nanowires exhibited either a single peak, ascribed to the wurtzite structure, or two distinct peaks, implying the simultaneous presence of both wurtzite and zinc-blende structures. It should be noted that the spectra had no observable contribution from luminescence that could be attributed to defects (stacking faults or impurity-mediated), which indicated high-quality samples. The observed CL spectrum, shown in Figure 2, indicates the coexistence of zinc-blende and wurtzite structures in a single isolated GaN nanowire. The peak maxima, observed at ∼3.64 and ∼3.88 eV, are identified as the zinc-blende and wurtzite peaks based on their similarity to those observed for bulk GaN. The energy band gap values for bulk GaN are 3.2 eV in zinc-blende[20] and 3.39 eV in wurtzite.[21] The increase in energy of 0.45−0.5 eV, measured by CL, may be attributed to both electron confinement and strain effects as discussed below.

The nanowire structure was investigated with HRTEM (JEOL 2200FS). Selected area electron diffraction (SAED) and fast Fourier transforms (FFTs) of the HRTEM images were used to identify the crystalline phases present. Energy dispersive X-ray spectroscopy (EDS) and electron energy loss spectroscopy (EELS) were used to investigate the elemental composition of the nanowires.

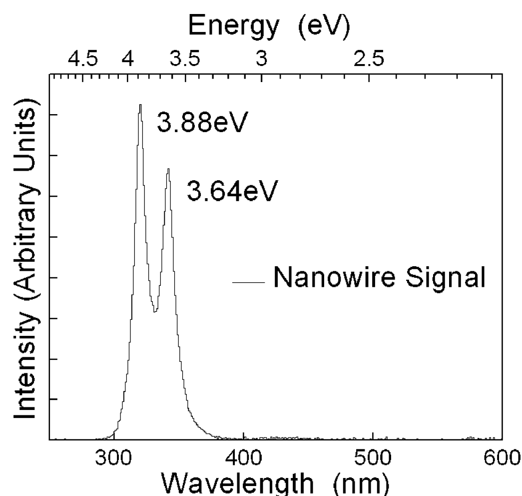

Figure 2. Cathodoluminescence spectrum showing the double peak indicating the wurtzite and zinc-blende phases present in the nanowire. The band gap energies for each phase is blue-shifted on the order of 0.45−0.5 eV.

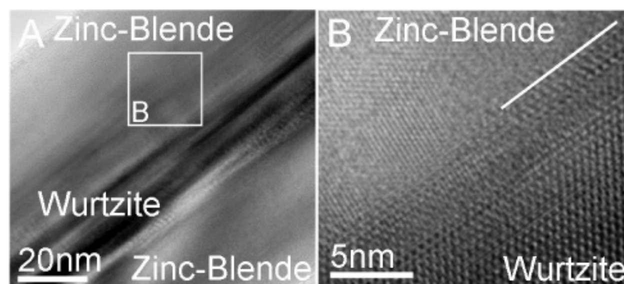

Figure 3. (A) TEM image of GaN nanowire showing the inner wurtzite phase, dark contrast, and the outer zinc-blende phase, lighter contrast areas surrounding. The white box indicates where the close up, image (B), was taken. (B) HRTEM image of the wurtzite/zinc-blende interface. The white line highlights where the phase transition occurs. This image also shows the highly crystalline nature of both phases.

A typical TEM image showing the full nanowire width is shown in Figure 3A. Analysis of multiple nanowires has indicated that the two-phase structure spans the entire length of the nanowire. A typical TEM and HRTEM image, shown in Figure 3A,B, indicates a sharp transition of ∼1−3 atomic layers between phases. Figure 3B also shows the highly crystalline nature of both phases.

SAED patterns were used to prove the biphasic structure of the nanowire, as shown in Figure 4. Both wurtzite phase and zinc-blende phase diffraction patterns were solved and confirmed with FFTs in the same areas where the SAED patterns were taken. The FFTs and SAED patterns were checked using JAVA electron microscopy simulation (JEMS) and were shown to be consistent with identifications. Diffraction spots from both phases when imaged together were also noted, and two such examples are indicated by arrows in Figure 4E. The growth direction of the nanowire shown in Figure 4 is in the [110] direction for the wurtzite phase, and in the [011] direction for the zinc-blende phase.

EELS and EDS spectra were taken to investigate the purity of the two crystalline phases by checking for the presence both gallium and nitrogen and the lack of oxygen. The

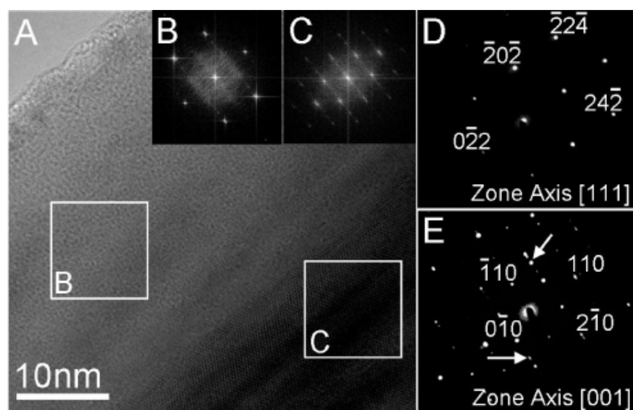

Figure 4. (A) HRTEM image indicating where the FFTs and diffraction patterns were taken, as shown by the white boxes. (B) FFT of the indicated area from (A). (C) FFT of the indicated area from (A). (D) Indexed diffraction pattern for the zinc-blende phase. The growth direction is [011]. (E) Indexed diffraction pattern for the wurtzite phase. The growth direction is [110]. Arrows indicate additional diffraction contributing from the zinc-blende phase.

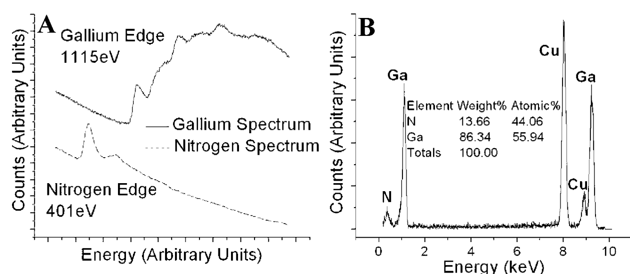

Figure 5. (A) EELS spectrum showing the nitrogen edge at 401 eV and the absence of an oxygen edge at 532 eV, lower spectrum. EELS spectrum showing the gallium edge at 1115 eV, upper spectrum. (B) EDS spectrum showing the peaks for both gallium and nitrogen. This is indicative of the 1:1 stoichiometry of the nanowire as shown in the table. The copper peaks are present due to the copper TEM grid.

presence of oxygen in GaN nanowires has been reported.[22] However, to achieve GaN nanowire growth by the method employed here, oxygen should be carefully eliminated from the starting materials. An EELS spectrum indicating a strong nitrogen edge at 401 eV and the absence of an oxygen edge at 532 eV is shown in Figure 5A. An EELS spectrum indicating a broad gallium edge at 1115 eV is also shown in Figure 5A. The atomic ratio of gallium to nitrogen was calculated using quantitative EDS and indicated a nearly 1:1 ratio of each element, as shown in Figure 5B. Both EELS and EDS confirmed no detectable presence of oxygen in these nanowires. The biphasic crystallographic orientations were therefore interpreted as two phases of exclusively gallium and nitrogen in equal quantities.

The majority of reports on GaN nanowire fabrication and structural characterization indicate that the nanowires have a pure wurtzite crystalline structure.[23,24] There have also been reports of GaN nanowires with a pure zinc-blende structure,[25] as well as reports where a mixture of wurtzite and zinc-blende phases is observed.[26,27] The possibility that our GaN nanowires were pure phase materials was investigated. The wurtzite diffraction pattern identification was checked against theoretical values for multiple diffraction planes for both [111] zinc-blende and the [001] wurtzite zone axes, as these patterns are very similar. As diffraction spots were measured further from the transmission spot, values corresponding to the [111] zinc-blende zone axis deviated substantially from ideal values, while values for the [001] wurtzite zone axis did not. The zinc-blende identification was further confirmed by the observation of [001] diffraction patterns (not shown) in addition to the [111] diffraction pattern, as shown in Figure 4D.

The basic catalyst-free nanowire growth mechanism of GaN involving the development of hexagonal crystallite platelets from an initial amorphous layer parallels the development of the nucleation layer observed in GaN thin film growth.[28] Gallium is sourced from subsequent matrix decomposition, resulting first in platelet growth, then as a kinetic equilibrium of growth and decomposition that maintains platelet size. Decomposition of a nucleation layer starts at ~800 °C for GaN on sapphire, in good accord with the temperature for onset of GaN nanowire growth in these present experiments. Gallium atoms are highly mobile on GaN surfaces[29] and are expected to diffuse rapidly along platelets and nanowires. Surface incorporation of Ga and NH_3 to form GaN has been modeled both theoretically[30,31] and experimentally.[32] NH_3 appears to undergo a barrierless chemisorption on GaN, leaving NH_2[33,34] and H.[35,36] However, nitrogen incorporation occurs only at step edges.[37] Therefore nanowire growth occurs at the tip leading edge. We have seen no evidence for a wurtzite core growth followed by subsequent zinc-blende shell growth. We therefore conclude that, for our experimental conditions, both phases grow together along the length of the nanowire through gallium and nitrogen incorporation at the tip leading edge following a biphasic pattern initiated during early nanowire growth.

A 0.45−0.5 eV band gap shift was observed in the CL measurements. An electron confinement calculation for the nanowires based on an infinite potential well model accounts for only a few meV of the observed band gap shift. Calculations based on experiment for pure wurtzite GaN nanowires have identified band gap shifts as high as 0.3 eV due to compressive and tensile stresses.[38,39] Therefore the band gap shift observed in the present experiments may have more contribution from stress than from electron confinement.

To summarize, we have reported evidence for a new biphasic crystalline homostructure in GaN nanowires based on the analysis by CL and HRTEM with SAED, FFT, EDS, and EELS. An inner wurtzite phase and outer zinc-blende phase crystal homostructure with a sharp phase transition of ~1−3 atomic layers has been observed. The ability to grow this biphasic GaN nanowire with longitudinal separation of defect-free zinc-blende and wurtzite phases is a new phenomenon. Biphasic nanowires based on longitudinal phase separation in heterostructures,[40] and now in homostructures, represent a new class of electron waveguide structures with important applications in quantum transport.

Acknowledgment. The support of NASA Goddard Space Flight Center, MEI Task no. 14, and the National Science Foundation PREM, CREST, and REU programs are grate-

fully acknowledged. One author (B.W.J.) would like to thank the NASA Goddard Graduate Student Researchers Program. Helpful discussions with K. P. O'Donnell are gratefully acknowledged.

References

(1) Nam, C. Y.; Jaroenapibal, P.; Tham, D.; Luzzi, D. E.; Evoy, S.; Fischer, J. E. *Nano Lett.* **2006**, *6*, 153−158.

(2) Johnson, J.; Choi, H. J.; Knutson, K. P.; Schaller, R. D.; Yang, P.; Saykally, R. J. *Nat. Mater*. **2002**, *1*, 106−110.

(3) Huang, Y.; Duan, X.; Cui, Y.; Lieber, C. M. *Nano Lett.* **2002**, *2*, 101−104.

(4) Huang, Y.; Duan, X.; Cui, Y.; Lauhon, L. J.; Kim, K. H.; Lieber, C. M. *Sci.* **2001**, *294*, 1313−1317.

(5) Cha, H. Y.; Wu, H.; Chandrashekhar, M.; Choi, Y. C.; Chae, S.; Koley, G.; Spencer, M. G. *Nanotechnology* **2006**, *17*, 1264−1271.

(6) Wu, H.; Cha, H. Y.; Chandrashekhar, M.; Spencer, M. G.; Koley, G. *J. Electron. Mater.* **2006**, *35*, 670−674.

(7) Nam, C. Y.; Kim, J. Y.; Fischer, J. E. *Appl. Phys. Lett.* **2005**, *86*, 193112.

(8) Tham, D.; Nam, C. Y; Fischer, J. E. *Adv. Mater.* **2006**, *18*, 290−294.

(9) Nam, C. Y.; Tham, D.; Fischer, J. E. *Nano Lett.*, **2005**, *5*, 2029−2033.

(10) Chen, X.; Xu, J.; Wang, R. M.; Yu, D.; *Adv. Mater*. **2003**, *15*, 419−421.

(11) Lee, S. K.; Choi, H. J.; Pauzauskie, P.; Yang, P.; Cho, N. K.; Park, H. D.; Suh, E. K.; Lim, K. Y.; Lee, H. J. *Phys. Status Solidi B* **2004**, *241*, 2775−2778.

(12) Han, W.; Fan, S.; Li, Q.; Hu, Y. *Science* **1997**, *277*, 1287−1289.

(13) Duan, X. F.; Lieber, C. M. *J. Am. Chem. Soc*. **2000**, *122*, 188−189.

(14) Zhang, J.; Zhang, L. *J. Vac. Sci. Technol*., *B* **2003**, *21*, 2415−2419.

(15) Bertness, K. A.; Roshko, A.; Sanford, N. A.; Barker, J. M.; Davydov, A. V. *J. Cryst. Growth* **2006**, *287*, 522−527.

(16) Nam, C. Y.; Tham, D.; Fischer, J. E. *Appl. Phys. Lett*. **2004**, *85*, 5676−5678.

(17) He, M.; Zhou, P.; Mohammad, S. N.; Harris, G. L.; Halpern, J. B.; Jacobs, R.; Sarney, W. L.; Salamanca-Riba, L. *J. Cryst. Growth* **2001**, *231*, 357−365.

(18) He, M.; Minus, I.; Zhou, P.; Mohammad, S. N.; Halpern, J. B.; Jacobs, R.; Sarney, W. L.; Salamanca-Riba, L.; Vispute, R. D. *Appl. Phys. Lett*. **2000**, *77*, 3731−3733.

(19) El Ahl, A. M. S.; He, M.; Peizhen, Z.; Harris, G. L.; Salamanca-Riba, L.; Felt, F.; Shaw, H. C.; Sharma, A.; Jah, M.; Lakins, D.; Steiner, T.; Mohammad, S. N. *J. Appl. Phys.* **2003**, *94*, 7749−7756.

(20) Lei, T.; Moustakas, T. D.; Graham, R. J.; He, Y.; Berkowitz, S. J. *J. Appl. Phys.* **1992**, *71*, 4933−4943.

(21) Maruska, H. P.; Tietjen, J. J. *Appl. Phys. Lett.* **1969**, *15*, 327−329.

(22) Peng, H. Y.; Wang, N.; Zhou, X. T.; Zheng, Y. F.; Lee, C. S.; Lee, S. T.; *Chem. Phys. Lett.* **2002**, *359*, 241−245.

(23) Cheng, G. S.; Zhang, L. D.; Zhu, Y.; Fei, G. T.; Li, L.; Mo, C. M.; Mao, Y. Q. *Appl. Phys. Lett.* **2006**, *75*, 2455−2457.

(24) Xue, C.; Wu, Y.; Zhuang, H.; Tian, D.; Liu, Y.; Zhang, X.; Ai, Y.; Sun, L.; Wang, F. *Physica E* **2005**, *30*, 179−181.

(25) Han, W. Q.; Zettl, A. *Appl. Phys. Lett.* **2002**, *81*, 5051−5053.

(26) Tham, D.; Nam, C. Y.; Fischer, J. E. *Adv. Funct. Mater.* **2006**, *16*, 1197−1202.

(27) Tham, D.; Nam, C. Y.; Byon, K.; Kim, J.; Fischer, J. E. *Appl. Phys. A* **2006**, *85*, 227−231.

(28) Wikenden, A. E.; Wickenden, D. K.; Kietenmacher, T. J. *J. Appl. Phys.* **1994**, *75*, 5367−5371.

(29) Zywietz, T.; Neugebauer, J.; Scheffler, M.; Northrup, J.; Van de Walle, C.G. *MRS Internet J. Nitride Semicond. Res.* **1999** *3S261*, G3.68.

(30) Fritsch, J.; Sankey, O. F.; Schmidt, K. E.; Page, J. B. *Surf. Sci.* **1999**, *428*, 298−303.

(31) Northrup, J. E.; Di, Felice, R.; Neugebauer, J. *Phys. Rev. B* **1997**, *56*, R4325−R4328.

(32) Brown, J. S.; Koblmueller, G.; Wu, F.; Averbeck, R.; Riechert, H.; Speck, J. S. *J. Appl. Phys.* **2006**, *99*, 074902.

(33) Bermudez, V. M. *Chem. Phys. Lett.* **2000**, *317*, 290−295.

(34) Pignedoli, C. A.; Di, Felice, R.; Bertoni, C. M. *Phys. Rev. B* **2001**, *64*, 113301.

(35) Gherasoiu, I.; Nikishin, S.; Temkin, H. *J. Appl. Phys.* **2005**, *98*, 053518.

(36) McGinnis, A. J.; Thomson, D.; Davis, R. F.; Chen, E.; Michel, A.; Lamb, H. H. *Surf. Sci.* **2001**, *494*, 28−42.

(37) Held, R.; Ishaug, B. E.; Parkhomovsky, A.; Dabiran, A. M.; Cohen, P. I. *J. Appl. Phys.* **2000**, *87*, 1219−1226.

(38) Seo, H. W.; Bae, S. Y.; Park, J.; Yang, H. N.; Park, K. S.; Kim, S. *J. Chem. Phys*. **2002**, *116*, 9492−9499.

(39) Kuykendall, T.; Pauzauskie, P. J.; Zhang, Y.; Goldberger, J.; Sirbuly, D.; Denlinger, J.; Yang, P. *Nat. Mater.* **2004**, *3*, 524−528.

(40) Lauhon, L. J.; Gudiksen, M. S.; Wang, D.; Lieber, C. M. *Nature* **2002**, *420*, 57−61.

NL062871Y